FoDTEC final summary report

Author: Tim Warren
Date: 07/05/2020
Reference: FT-008
Version: A

Approval / Revision History

Version	Date	Changes	Author	Checked	Approved
A	07/05/2020	Initial Issue	TW	JP	TW

Interreg North-West Europe FORESEA
European Regional Development Fund

Contents

1 References

Ref 1. FT-010: Biofouling Survey report for FoDTEC, Want, A. Porter, J.S, April 2020

Ref 2. FT-009. Forensic examination of material deriving from the TGL tripod, Anguilano, L. Karim, M. Minton, T. McKay, B. Nelson, N. April 2020

Ref 3. 20190711_EMEC_Scaled.ply. ROVCO 3D point cloud Model

Ref 4. 093642, 094642, 095643, 100642, 101642, 102642, 153050, 152350: ROVCO ROV survey video footage (07/11/2019)

2 Acronyms

CAD – Computer Aided Design

DGIII – DEEP-Gen III turbine (first generation 500kW tidal turbine that was deployed by TGL)

DGIV – DEEP-Gen IV turbine (second generation 1MW tidal turbine deployed by RR/Alstom)

EBSD – Electron back scattering diffraction

EMEC – European Marine Energy Centre, based in Orkney

FoDTEC – Forensic Decommissioning of Tidal Energy Converters

FORESEA - Funding Ocean Renewable Energy through Strategic European Action

ICIT - International Centre for Island Technology

OEC – Ocean Energy Converter

ROV – Remotely Operated Vehicle

TGL -Tidal Generation Limited

3 Executive Summary

After the removal of the TGL tidal turbine foundation that was installed at EMEC's Fall of Warness tidal test site, the FoDTEC project has completed activities to assess biofouling, corrosion, metallurgical defects and electrical connector longevity. Work has been completed by the following partners in the project:

- Blackfish Engineering Design Ltd: responsible for coordination of inspection activities, as well as visual inspection and data collection
- Brunel University, responsible for metallurgical assessment
- Herriot Watt University, ICIT, responsible for bio-fouling assessment
- ROVCO, responsible to ROV survey and subsequent 3D imagery.
- EMEC, responsible for managing the tripod removal.

The project has consisted of the following activities:

- Tripod removal from seabed and transport to sheltered location.
- Diver and ROV biofouling survey conducted by ICIT
- ROV scanning survey conducted by ROVCO, to create a replica 3D CAD model of the tripod
- Cut up and removal of the tripod onto Hatston Quay
- Photo survey and assessment of biofouling and corrosion
- Removal of cartridge plate and electrical connectors for further assessment
- Tripod sample cut-out and removal for detailed metallurgical assessment by Brunel University

The main objectives of the project were:

- To develop a process of data collection to obtain a comprehensive understanding of the end-of-life condition of Ocean energy Converter (OEC) devices
- Validate this service through its execution in a relevant OEC decommissioning project.
- Validate ICIT's system for the monitoring of biofouling on OEC devices, through its implementation in a relevant environment.
- Develop guidelines for material specification to respond to the combination of marine and fatigue corrosion.
- Present the collected and analysed data in a suitable format for dissemination to the wider OEC industry.

This report provides an overall summary of the work completed. More detailed reports of the activities completed by individual companies can be found in the references.

All partner companies have been able to develop their services of providing analysis in their respective specialist fields and have provided recommendations and lessons learned regarding provision of the services.

4 Background and Introduction

The FoDTEC (Forensic Decommissioning of Tidal Energy Converter) project, funded through Interreg North West Europe's FORESEA programme, has been set up in order to facilitate the removal of the Tidal Generation Ltd support foundation that was installed in the Fall of Warness site at EMEC and to conduct detailed assessment of biofouling, corrosion, metallurgical defects and other visual evidence.

FORESEA is an €11m project which has helped to bring offshore renewable energy technologies to market by providing free access to a world-leading network of test centres: the European Marine Energy Centre (EMEC) (UK), SEM-REV (France), SmartBay (Ireland) and the Dutch Marine Energy Centre (Netherlands). Access is awarded through a series of competitive calls for application. It is financed by the Interreg North West Europe programme.

www.foreseaproject.eu

The aim of the project is to provide feedback and design guidelines to the offshore renewable energy industry to improve the design of marine energy converters in relation to biofouling, corrosion protection, and the effects of long term submersion in seawater.

The tripod foundation was installed at EMEC in summer 2008 and removed in October 2019. It has therefore been submerged in a high flow tidal site for approximately 11 years. During that time, 2 tidal turbines have operated on it, the Tidal Generation Ltd (TGL) 500kW and 1MW turbine (ReDAPT). In total, over 1250 MWhrs of electricity were generated to the grid over a period of 7 years.

Figure 1 - 500kW and 1MW (ReDAPT) turbines

The tripod was installed at the EMEC Fall of Warness site, with flood and ebb flow bearings of 170 and 347 degrees. As a guide, the J-tube was pointing roughly into the flood tide (NNW).

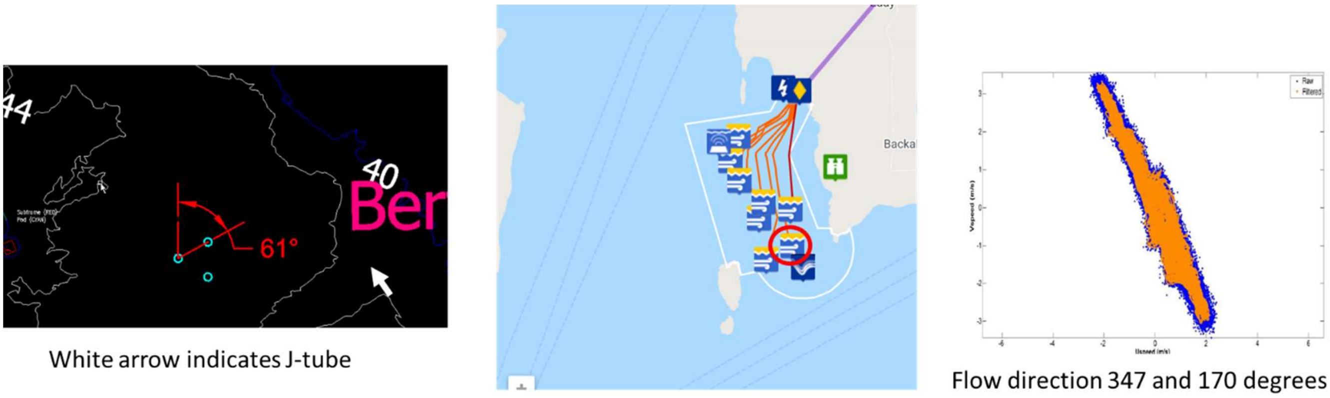

Figure 2 – Left - Tripod feet locations and angles, Centre - EMEC berths (centre) and right - flow velocity (northings and eastings)

Figure 3 - Tripod as installed in 2008

The tripod feet were cut through in summer 2019, and the tripod left in place for a few months after that. It was moved to shallow water (near Eday) approx. 4 weeks prior to the biofouling survey and subsequent recovery on 19/10/2029. The tower top was cut off and removed prior to being moved to shallow water, as the tripod was too tall for the water depth. This was recovered to the yard of Leask Marine in September 2019. The tripod was finally lifted from the water and placed on Hatston Quay for 24-hour inspection window on 15/11/2029 prior to being scrapped.

Where high resolution pictures are available, larger versions have been placed in Appendix B for reference.

5 Summary of Biofouling survey work by ICIT

A full record of the work completed has been documented in Ref 1. A summary is presented here.

Marine operations conducted by Leask Marine provided 3 opportunities to survey biofouling during the decommissioning process:

a) Diver survey – at a temporary, shallow-water location adjacent to the Fall of Warness – 25 June 2019. Samples were collected from each of the tripod legs and the central vertical support for later study
b) Tower top survey– at Leask Marine yard, Hatston – 15 September 2019. Survey was limited to photographic evidence only
c) Remaining tripod survey – at Hatston Pier, shortly after recovery to land – 6 November 2019. The team employed a rapid assessment survey approach to list all species and abundances on sight, as well as photographing representative quadrats (25 x 25 cm) (Figure 6) and all fouling material removed and collected by scraping the samples into a sealable bag for later analysis

Note: following removal of the vertical subunit at the temporary, shallow-water location adjacent to the Fall of Warness, the remaining tripod was towed to shallow seas at Hatston on 22 October 2019.

5.1 Data analysis:

Certain small species, not easily identifiable in the field, and samples collected during the diver surveys were identified in the laboratory under a low power microscope. Samples of particular significance, e.g. rare species, were preserved in 70% ethanol for voucher material to be deposited in an appropriate repository for long-term curation.

Quadrat images were analysed for percent cover of key fouling species using the 'Cover-Up' software programme. In this application, 100 'dots' were generated and randomly placed over each image. Identification of biofouling species beneath each 'dot' was tallied to provide quantified assessment of fouling abundances.

Estimates of total fouling weight were determined by obtaining wet and dry weight of samples collected by representative quadrat scrapes. Dry weight was determined after samples were placed in a drying oven and weighed at intervals and until their weights stabilised.

5.2 Results:

Diver survey: 30 species (22 sessile; 8 motile) were identified from the samples collected during the dive survey. The most dominant foulant was the large barnacle *Chirona hameri*. Other organisms which were present on all four sampled components of the tripod were saddle oysters (e.g. *Anomia ephippium*), skeleton shrimp (*Caprella* spp.), the bryozoan

Callopora lineata, colonial sea-squirts (*Diplosoma* spp.), the amphipod *Jassa falcata*, and the common mussel (*Mytilus edulis*).

Samples collected during the diver survey at the uppermost portion of the tripod (i.e. in the shallowest water) included juvenile samples of algae and kelp. These photosynthetic plants are certain to have settled and grown only in the approximately 4-week period after removal from the deep water site.

Tower top survey: this structure was almost entirely covered in biofouling organisms creating a complex matrix extending typically 8-10cm but in places to over 12 cm in thickness (Figure 5). The dominant species were *Chirona hameri*, *Mytilus edulis*, and a wide variety of sponges, especially underneath features. Significant fouling was observed of saddle oysters, a turf of hydroids, and the barnacle *Balanus balanus*. Biofouling of structures placed in the marine environment will undergo a series of successional changes, depending upon the season of deployment. Pioneering macrofouling is often associated with colonial hydroids. After prolonged deployment, larger and more slow-growth species may dominate fouling. Studies of the fouling assemblages on the TGL tripod reported here can be considered as indicative of 'end-stage' or 'climax' biofouling communities on steel in these habitats. Once these stages have been reached, the assemblages observed here would not be expected to change much over time, except for localised areas of disturbance. Reports from the oil and gas sector have identified similar fouling assemblages on long-term deployed infrastructure in the North Sea (Forteath *et al.*, 1982). Patches of thicker fouling versus exposed substrate indicate that some level of disturbance can and does occur, perhaps as the consequence of large sediment impact.

Remaining tripod survey: 29 species (16 sessile; 13 motile) were identified from the samples collected shortly after the remaining tripod was lifted onto Hatston Pier. As with the other surveys, the overall dominant fouling was by large barnacles, *Chirona hameri*. Survey of the whole structure allowed observation of clear zonation of fouling. Lower regions of the structure were heavily encrusted by sponges, predominantly on top of barnacles *Chirona hameri*; upper regions featured much higher abundance of large common mussel *Mytilus edulis* (Table 1). Based on these surveys, no quantifiable difference in fouling assemblages was apparent between the 3 legs. Wet and dry weights of fouling within representative quadrats are presented in Table 2. In general, the percent cover and weight of fouling was similar between zones. The mean dry weight of fouling per 625 cm^2 was 893.40 g. Extrapolated, this equates to 14.29 kg/m^2.

In total, 44 species were identified (Table 3). The presence of invasive species, non-native to Orkney waters, was not detected in any of these surveys. This is consistent with earlier studies published on biofouling communities observed in marine renewable energy test centres in these waters (Want *et al.*, 2017).

Zone	*Chirona*	*Porifera* spp.	*Mytilus*	*Hydroida* spp.	*Ophiothrix*
Upper	52	15	31	2	0
Middle	54	37	6	3	0
Lower	34	52	7	5	2

Table 1 - Percent cover of major fouling taxa from representative quadrats (25 x 25 cm)

Zone	Wet weight (g)	Dry weight (g)
lower	1365.32	820.22
mid	1381.82	946.15
upper	1413.99	913.84

Table 2 Wet and dry weights of representative quadrats (25 x 25 cm)

Amphilectus fucorum	*Chirona hameri*	*Majidae* spp.
Amphisbetia operculata	*Didemnum maculosa*	*Metridium dianthus*
Anomia ephippium	*Diplosoma* spp	*Mytilus edulis*
Aphroditinae spp.	*Echinus esculentus*	*Nematoda* spp.
Archidoris pseudoargus	*Electra pilosa*	*Nemertea* spp.
Asterias rubens	*Filograna implexa*	*Nereidae* spp.
Balanus balanus	*Gibbula cineraria*	*Ophiothrix fragilis*
Botryllus schlosseri	*Grantia compressa*	*Platyhelminthes* spp.
Bugulina flabellata	*Haplopoma graniferum*	*Polychaetae* spp.
Calliostoma ziziphynum	*Henricia oculata*	*Sarsia eximia*
Cancer pagarus	*Hiatella arctica*	*Spirobranchus triqueter*
Caprella spp.	*Jassa falcata*	*Sycon ciliatum*
Cellaporina hassalli	*Leuconia nivia*	*Trivia arctica*
Callopora lineata	*Leucosolenia* spp.	*Verruca stroemia*
Cellepora pumicosa	*Macropodia* spp.	

Table 3

Species observed on the tripod during decommissioning surveys

5.3 Conclusions

The diver survey was in a site with significant water flow, which restricted the time window available. In future, this should be in static water

Studies of the fouling assemblages on the TGL tripod reported here can be considered as indicative of 'end-stage' or 'climax' biofouling communities on steel in these habitats.

Patches of thicker fouling versus exposed substrate indicate that some level of disturbance can and does occur, perhaps as the consequence of sediment impact.

The presence of juvenile red and brown algae from the uppermost sampled portions of the tripod collected at the temporary, shallow-water sites are not indicative of the fouling community in deep, rapid currents where tidal turbines are expected to operate. Rather, these observations provide caution that if the objective is to study biofouling in as clear and systematic means as possible, the research partners must ensure that marine operations and biofouling surveys are coordinated to minimise subjecting infrastructure to contrasting environmental conditions.

No Non-Indigenous Species (NIS) from the infrastructure were identified on this survey. The fauna we documented is characteristic of a subgroup of known fouling species, which thrive in high current flow environments.

5.4 Lessons learned

- Diver surveys need to be completed in static water.
- Diver surveys need to be done as soon as possible, to prevent the growth of new biofouling species.
- If these studies are to be done in the future, then better coordination of marine operations and diver surveys is necessary to ensure timely surveys can be completed.
- More time on site is required to survey, identify and catalogue biofouling. The 24 hour window on the quayside was not sufficient to collect all the data.
- The quadrat method of assessing biofouling on different parts of a structure is a very quick and effective method of making comparisons.
- Design of subsea structures should account for the end stage biofouling thicknesses on all surfaces, taking into account any lifting, buoyancy effects, or dis-assembly.

ding

Figure 5 - The vertical subunit of the tripod surveyed on 15 September 2019. Note the thick encrustation of barnacles and mussels

Figure 6 Images of quadrats (25 x 25 cm) were collected from the recovered tripod.

6 Summary of Tripod ROV survey by ROVCO

This work completed is fully documented in Ref 3 and Ref 4. It is summarised below.

ROVCO were brought into this project after the initial kick-off, as their expertise in ROV surveying and the techniques that they have to create 3D images of ROV scans was deemed to be beneficial to the project.

ROVCO completed an ROV survey on 11.07.2019 and have processed the data to produce a 3D point cloud data model of the tripod. This is shown from various views and levels zoom in the images below.

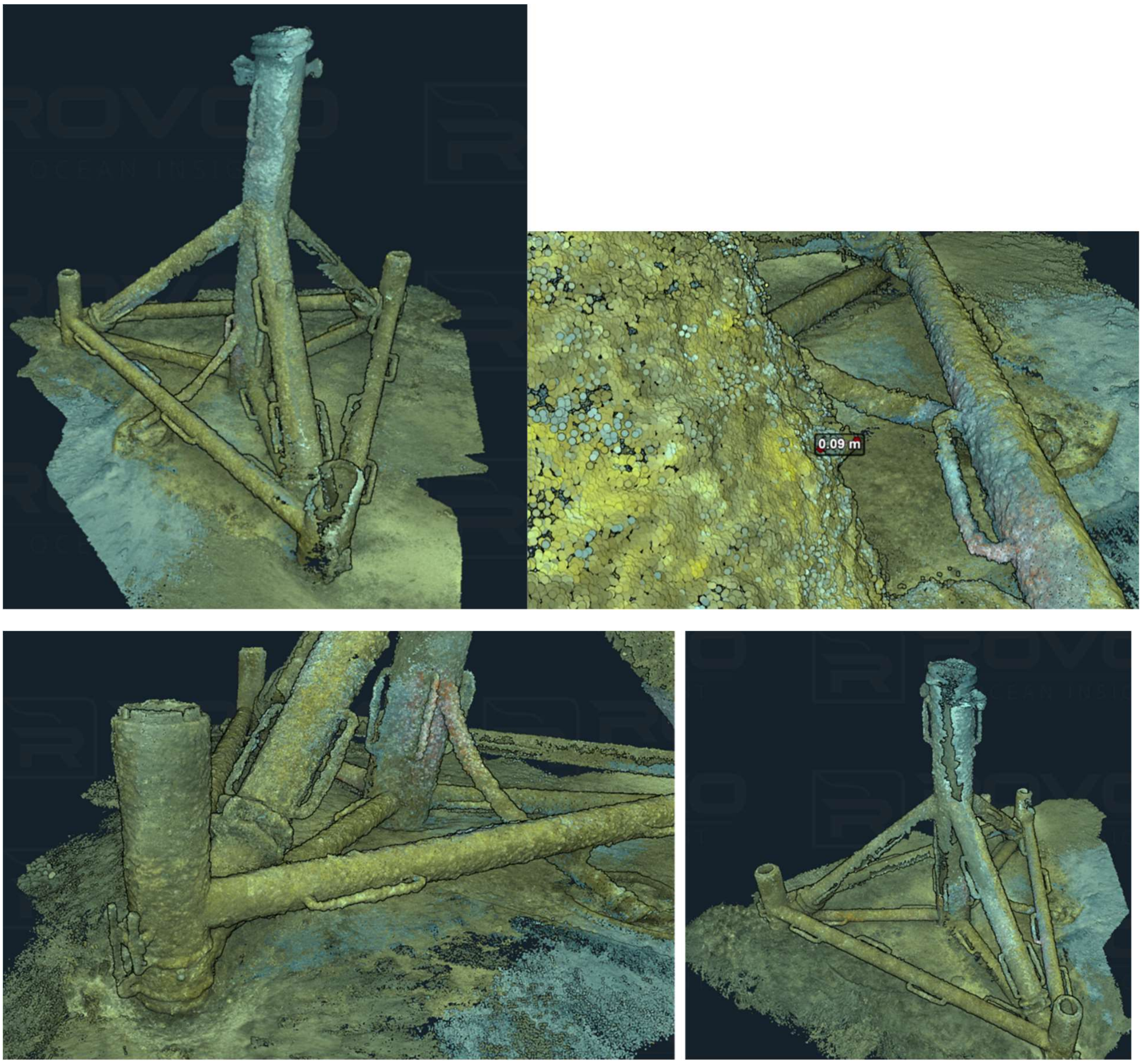

Figure 7 - 3D scanned point cloud data of underwater tripod, showing overview, a measured biofouling thickness and details of key features.

Some key observations:

- The 3D point cloud images provide excellent overview of the tripod, and it is clear that this technique can provide invaluable data for subsequent marine operations.
- Some point cloud data is missing, in particular on the underside and "inside" surfaces of the tripod members. This is due to restricted access of the ROV, as it is unable to fly under some members to view the underside.
- Analysis to determine the effects of tidal direction have not highlighted any particular results. This implies that flow speed in tidal sites is not too fast to prevent growth, nor is there any preference of biofouling to grow in higher or lower flow speed regions. This is corroborated by the biofouling survey and visual inspections
- Assessment to determine biofouling thickness has determined a large range of thicknesses. This is not particularly dependent upon flow direction.

6.1 Lessons learned

- The ROVCO scanning tool is an excellent method of providing advance knowledge of the condition of subsea hardware. ROV surveys can be difficult to interpret and the exact view of a feature of interest is not always possible. In particular, it can be difficult to get good resolution still images from the video with clear images of the area of interest.
- Preliminary measurements of biofouling thickness can be taken and correlate well with actual measurements.
- It is a quick a relatively inexpensive method of producing valuable data.

7 Comparison of ROV footage

ROV footage is available from:

- November 2010 – the tripod has been installed for 1 year, and this is shortly after initial deployment of the 500kW turbine.
- July 2017: Prior to planned tripod removal, and ROV survey was conducted. Actually, the tripod was not removed until October 2019.
- July 2019: Survey as part of the ROVCO work

The following images show a comparison of similar views and show directly how the biofouling has developed over that time. ROV footage is difficult to compare easily as lighting, turbidity and movement speed all affect the quality of the images, and it is impossible to get identical images from different surveys. The 2019 survey is not included, as the 3D images provide a much better view of the results and the biofouling is not much different to the 2017 survey (corroborating the "end stage" growth of the biofouling colonies).

Tower top

2010 2017

Tripod central node

2010 2017

J-tube with cable exit

2010 2017

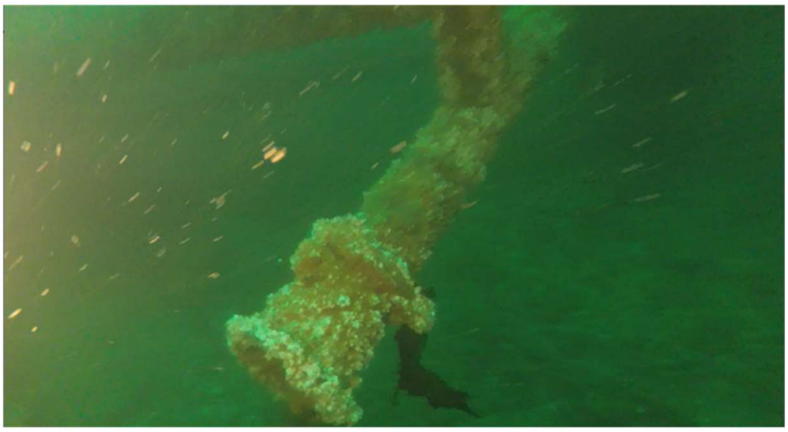

Tripod leg with grout lines

2010 2017

Tripod leg with stinger

2010 2017

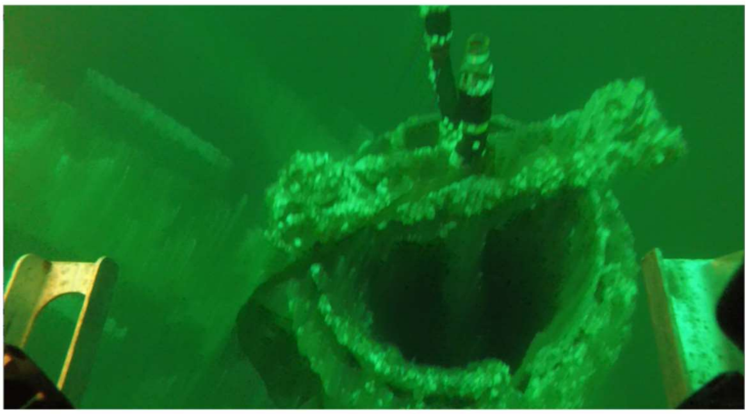

Figure 8 - ROV footage comparisons between 2010 and 2017

Specific conclusions form the ROV footage are difficult to draw, but it is clear that the biofouling has increased significantly over the time period. It is not possible to infer conclusions about directionality of the tidal flow and the effect on bio-fouling, but it is clear that biofouling is less dense where:

- Rubber hosing used as grout connections
- Sheltered internal volumes not directly exposed to flowing or highly oxygenated water
- Inside protected features, such as the J-tube

It is difficult to assess bio-fouling thickness from the survey and in many instances it is difficult to produce meaningful still photos from the video footage as the camera is moving too fast.

8 Summary of metallurgical assessments completed by Brunel University

All work completed by Brunel is documented in Ref 2

In summary, the objectives were to:

- Identify a protocol for sample selection and preparation to enhance the data for forensic investigation.
- Identify analytical techniques to obtain information on material changes and degradation.
- Characterise the material and link the observation to material properties, manufacturing, and use.

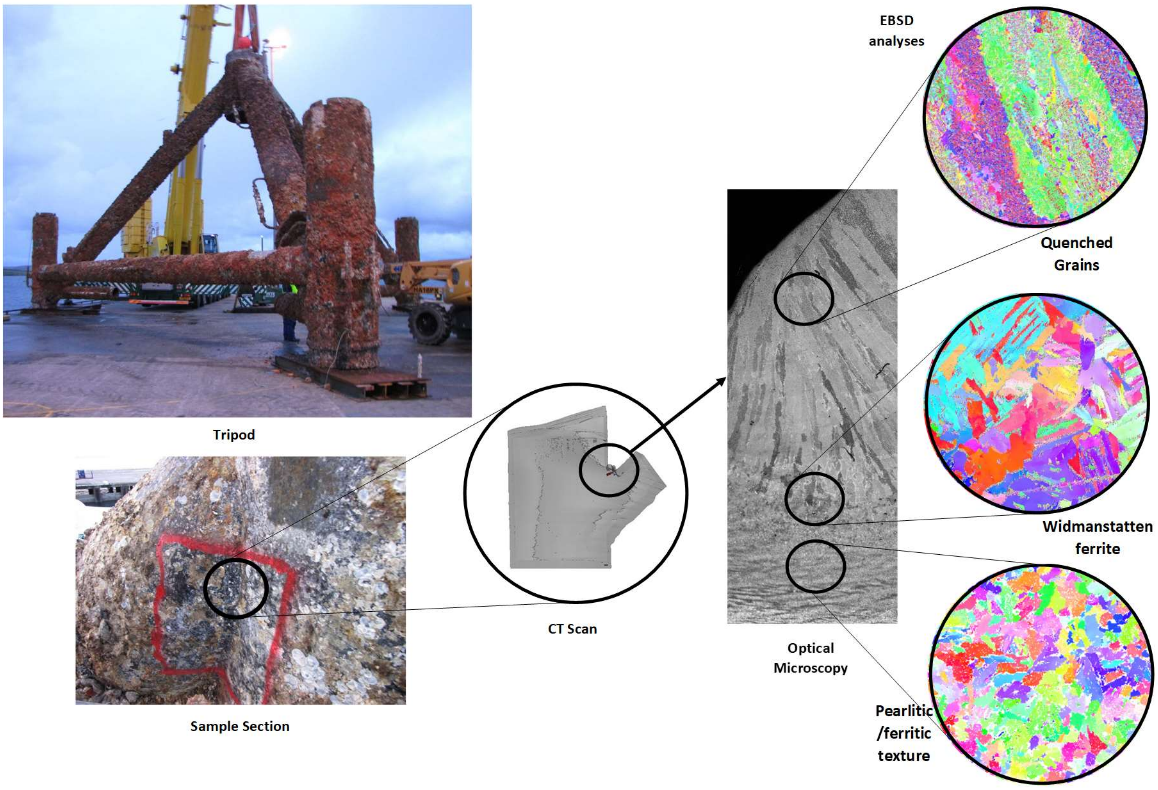

Figure 9 - Overview of analysis techniques

8.1 Methods used:

Sample selection: 15 samples for characterisation were highlighted, but in the event only 3 large sections were removed from the tripod due to time constraints. These were from the following locations:

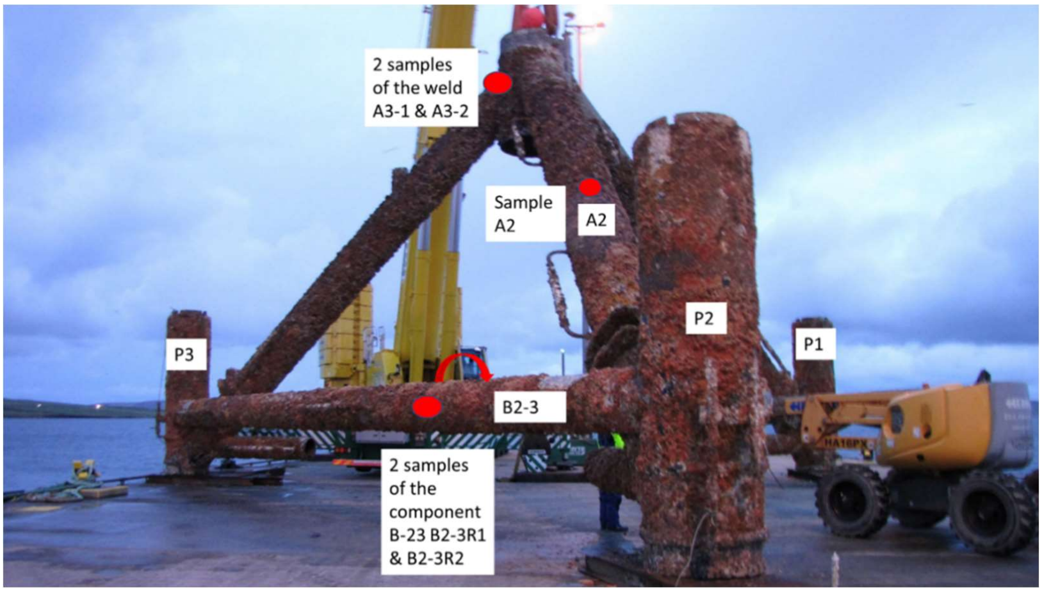

Figure 10 - Sample locations on tripod

Several methods of analysis were used.

a. stereo-microscope - The samples will be investigated to characterise areas of fracture/cracking, pitting, discolouration, in order to possibly identify areas of fracture initiation, failure mechanisms, corrosion phenomena.

Photographic evidence of the investigation was also collected.

b. Scanning electron microscope

b1. Scanning electron microscope on the sample as received was performed to investigate:

- fracture surfaces to identify failure mechanisms, initiation of the cracks and cracks propagation.
- pitting depths.
- corrosion products, their composition and their distribution.

After the screening of the corrosion a cleaning procedure was applied to investigate the metal surface underneath the corrosion layer and investigate the degree of alteration, depth of corrosion and level of damage.

b2. Scanning electron microscope on mounted samples

Sections of the sample were mounted in conductive resin for investigation of:

- chemical composition of the metal to evaluate if it is in specification;
- grain microstructure to evaluate if manufacturing and processing methods were applied according to specification;

b3. Electron back scattering (EBSD) of polished surfaces

Mounted samples underwent electron back-scattering analysis to evaluate orientation effects in the grains and deformations such as strained grains and twinning.

8.2 Results

8.2.1 Sample B2-3 R1 & R2

This sample showed a ferritic structure, determined using the indexing of the diffraction patterns obtained by EBSD, with randomly oriented (Figure 14) equiaxed grains of 10-20 µm size. Bands (highlighted in red in Figure 11) derived from the hot rolling are visible in the material without any deformation of the alignment. Furthermore, the random orientation observed (Figure 11 and Figure 14) indicates that heat treatment was performed after rolling to minimise the rolling effect and allow grain relaxation. Strain can be seen as internal misorientation ion the grains, but no strain was visible within the grains, any misorientation detected was due to sample preparation This can be ascertained looking at the variation of orientation (misorientation) within the grains and observing if this variation continues in the adjacent grain or not. If the misorientation can be seen in 2 or more adjacent grains than the variation is due to sample preparation, if it is confined within one grain then it is due to strain. Some porosity is visible in the sample (left hand side of Figure 11, white ellipsoidal points highlighted with blue circle), however they do not show any link with the exposed surface (i.e. they are not linked to pitting) and they do not show any deformation

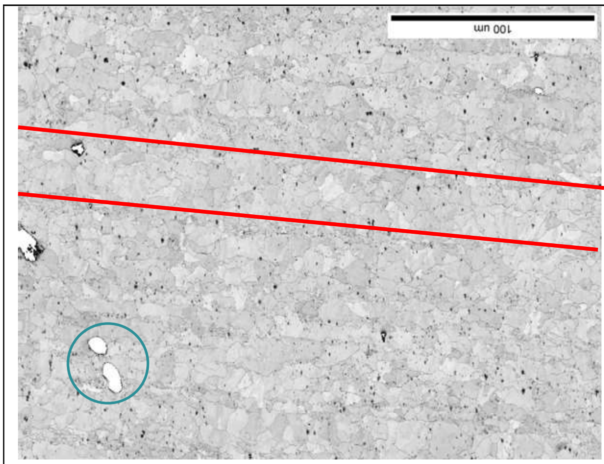

Figure 11 Image Quality map showing the banding phenomenon (highlighted in red) and some porosity (white ellipses in the left-hand corner)

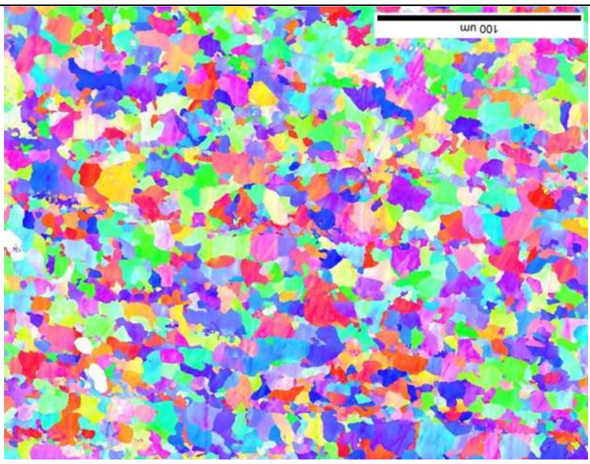

Figure 12 Inverse Pole Figure map showing the random orientation of the grains and the banding of smaller grains (perlites)

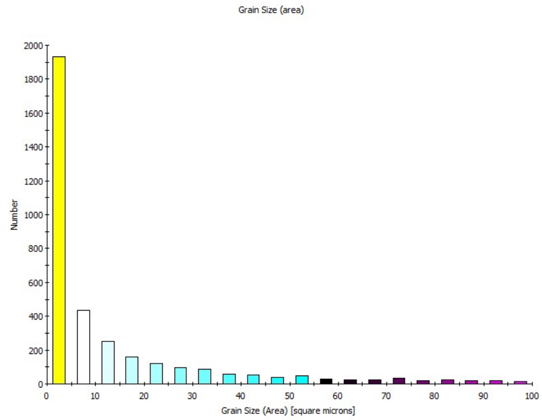

Figure 13 grain size chart indicating the smallest grains and then the range 10 to 50 and 50 to 100 in colour coded system represented in Figure 14

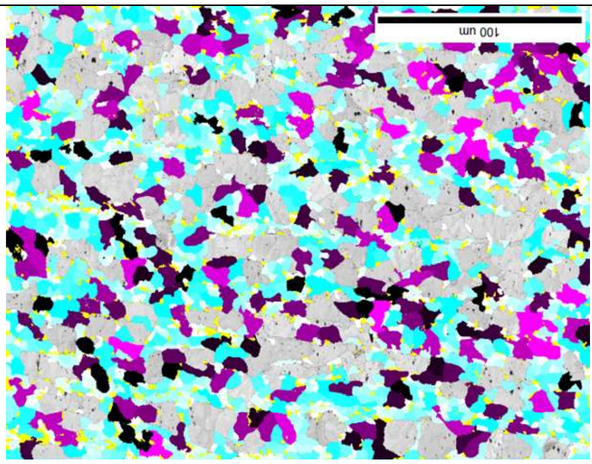

Figure 14 Image Quality map with colour coded grains depending on the size as per diagram Figure 13. Smallest grains in yellow are linked to perlites and show the banding phenomenon, larger grains are of ferritic nature

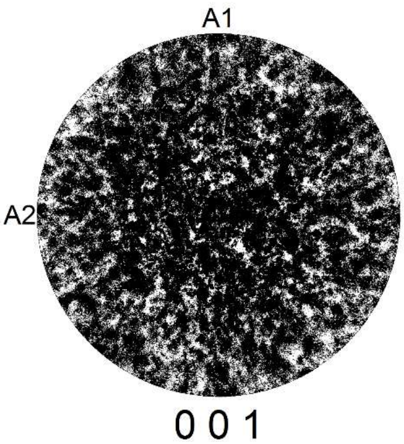

Figure 15 pole figure showing that no texture (preferential orientation) is visible in the sample.

8.2.2 Samples A1, A2, A3

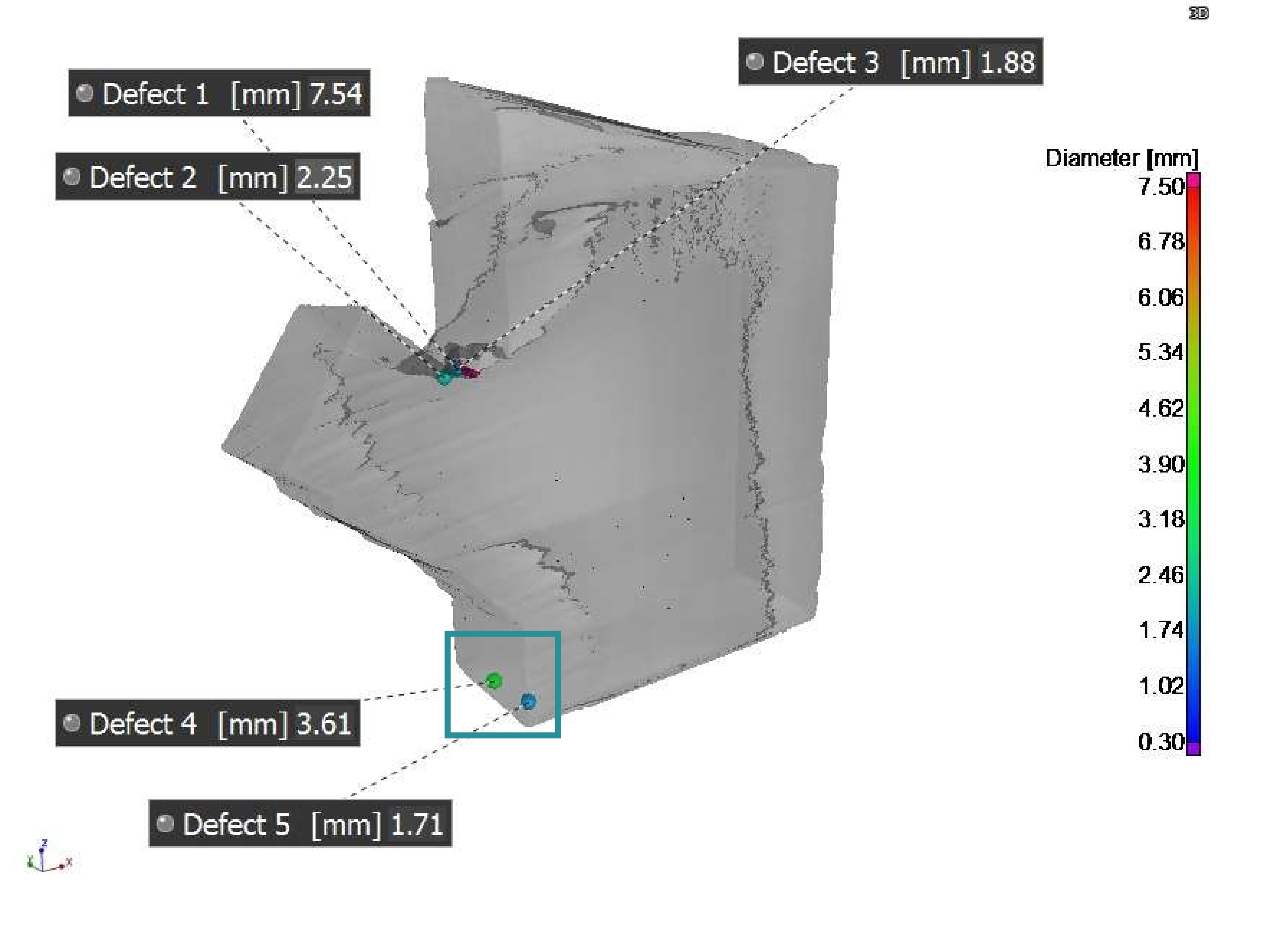

Figure 16 Side image of the CT scan highlighting defects and their size. 2 major groups of defects are visible: within the 3 points weld in the V shape area (defects 1-3), and at the bottom of the cross section (defects 4-5)

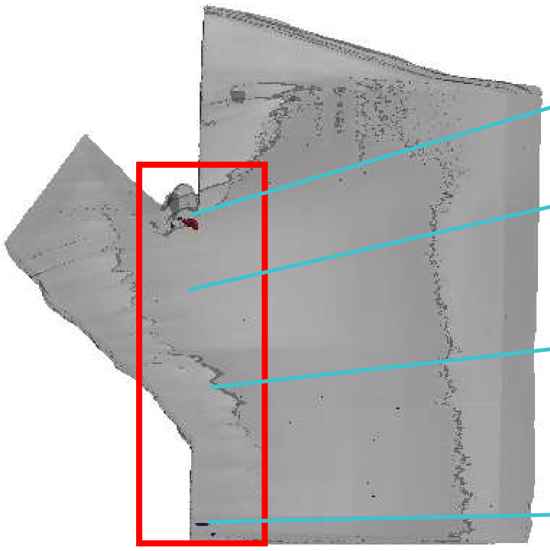

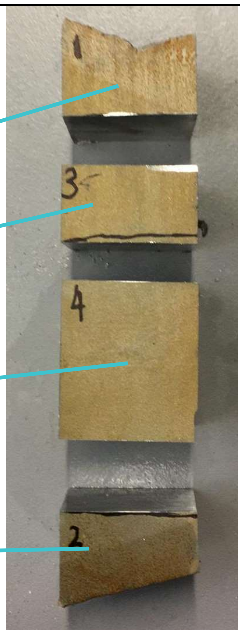

Figure 17Another side view from the CT scan. In red the section cut for analysis	Figure 18 Samples cut from the weld, and their labels. Arrows allow to locate the samples in the CT scan image

Area 1 (Figure 18) The optical microscopy observation shows a variation in the texture of the sample (elongated grains above the red line in Figure 19, Widmannstatten microstructure between the red and the green line and equiaxed grains below the green line). On the top elongated grains are visible, then a Widmannstatten microstructure can be observed with an area containing equiaxed grains beneath. Closer observation using electron microscopy on the top section (Figure 20, Figure 22and and Figure 24) indicated that the grain start recrystalising as elongated dendrites growing perpendicular to the top surface and are then quenched during the welding, and rapidly cooled provoking a large outer grain while on the inside very small single grains were formed (Figure 21). The specific orientation relationship between the finer grains in this top section is 47 degrees, which corresponds to the orientation relationship in the bottom section of this sample (below the red line) typical of body centre cubic ferritic iron under rapid conditions transforming the ferritic structure into a Widmannstatten one, generally present in welds and seams. This microstructure consists of intertwined lamellar grains, with a relationship similar to the one showed for twinnings, deriving from the fast cooling of austenitic grains produced in the ferritic steel by heating above the stability temperature of ferrite (which happens during welding) . Porosity is also visible in this area indicating (1) a decrease in volume of the material, which corresponds with the description of the twinning formation creating the Widmannstatten microstructure, as described by Cox (1954), (2) gas formation during the welding process. An evaluation of the strains in these areas was performed (Figure 23, Figure 24). The Kernel maps are shown in red the areas with higher strains. Analysing the results it can be noted that areas of major strains are the “shells” of the elongated grains in the welding areas (Figure 24), containing the finer grains deriving from the quenching process after welding. In detail (Figure 23) further strain is visible in the Widmannstatten area just below the elongated dendrites (below the red line in Figure 19, Figure 20, Figure 22) , while the strain decreases in the Widmannstatten area further below. This location of the strain and the associated location of the

porosity seem to point towards a phenomenon linked to the welding process more than with the use which could be expected to occupy a larger portion of the sample and not been limited to the heat affected zone of the welding itself.

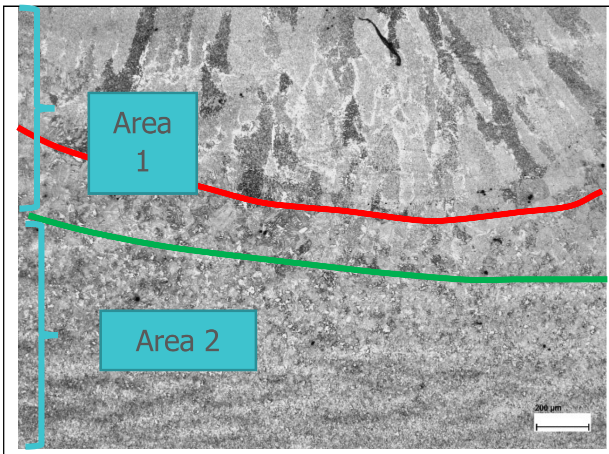

Figure 19 Optical microscope image of sample A3-1 showing the upper region of elongated grains towards the surface of the V shape area (Figure 17,Figure 18), above the red line. Between the red and the green line is the Widmannstatten area and below the green line the equiaxed ferritic/pearlitic zone.

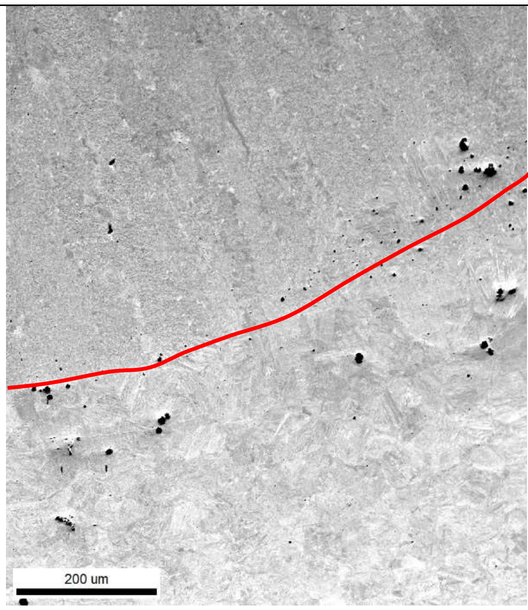

Figure 20 Forward scattering detector image of the sample showing the two distinct areas formed by elongated grains (above the red line) and Widmannstatten microstructure (below the red line

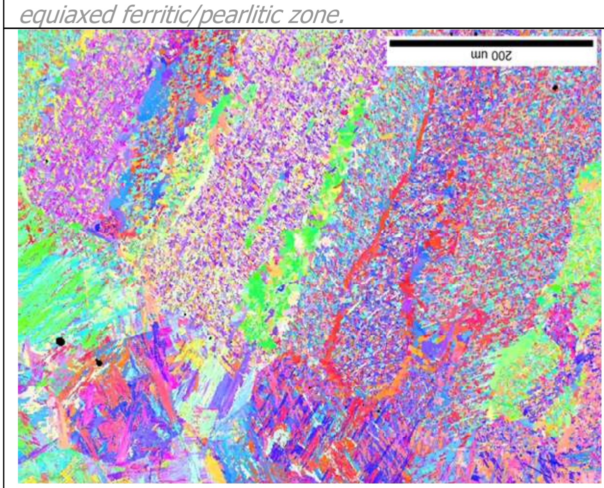

Figure 21 detailed view of the boundary between elongated grains and Widmannstatten area. It is visible here that the elongated grains are formed by minuscule

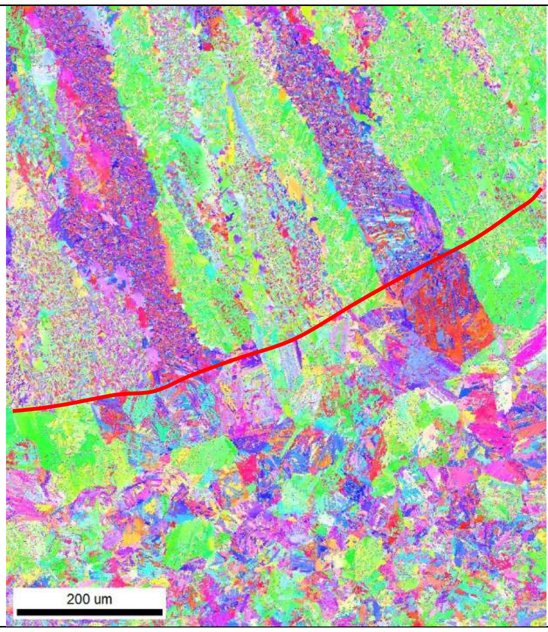

Figure 22 Corresponding IPF map of area in Figure 20 showing the orientation of the grains and the

grains with specific orientation and correlated to the orientation of the twinned grains below	*relationship between the orientations (analysis courtesy of Rene de Kloe – EDAX/Ametek)*
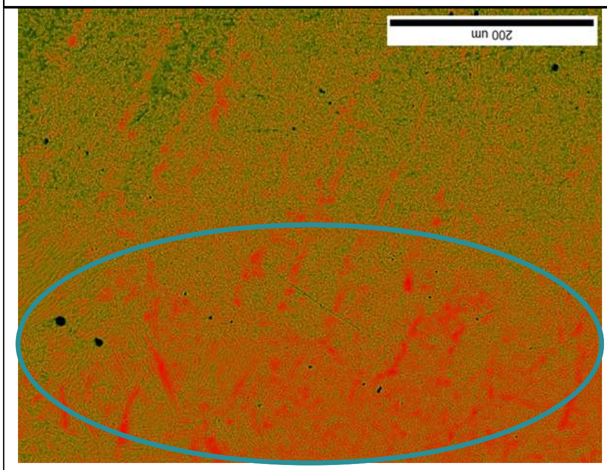	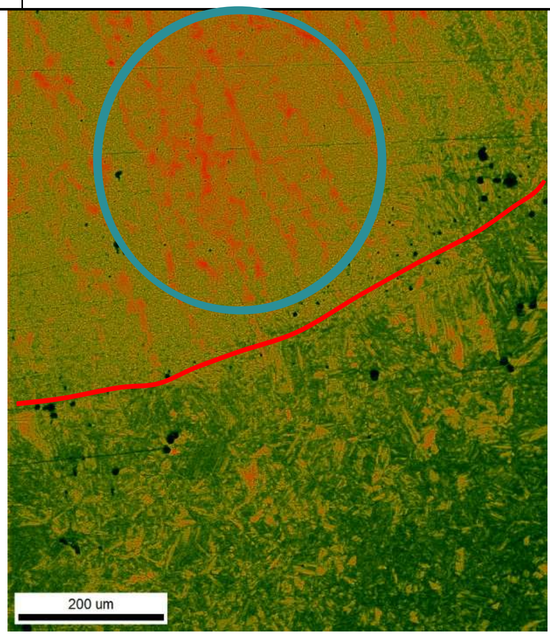
Figure 23 Kernel average map of Figure 22showing the maximum strain along the edges of the elongated grains at the boundary Widmannstatten zone and on the upper layer of the twinned zone (circled in blue)	*Figure 24 Kernel average map of Figure 20Figure 22a and b showing the maximum strains at the boundary of the elongated grains (circled in blue). Visible porosity along the line limiting elongated and the Widmannstatten area . (analysis courtesy of Rene de Kloe – EDAX/Amete*

8.3 Conclusions

A comprehensive metallographic evaluation of samples deriving from the tripod was performed to investigate potential changes in the material due to use. The main conclusions are summarised below:

Investigation of the samples indicated that no pitting occurred in the material, no cracks or porosity were visible from the surface inwards. Some porosity was visible in the samples, potentially due to manufacturing, however the porosity did not initiate cracks

The sample A3-1 shows a microstructure with evidence of overheating, as expected in a welding area, with a fine grained quenched top layer and a Widmannstatten area just below. The presence of porosity and the fact that the Widmannstatten microstructure is harder and more brittle, could have caused failure in the material and high strain concentration. However, fact that the porosity is not deformed seem to indicate that the microstructure is convincingly the result of the welding process more than the response of the stresses during use, and no fractures or fatigue corrosions were initiated in this areas.

Overall, all the features observed in the material appear to be linked to manufacturing, while no changes due to use were detected in the component. No impact of deployment was visible in the selected samples, hence indicating that for this component the deployment did not provoke any damage to the material.

8.4 Lessons learned and recommendations

- Despite not finding evidence of material defects due to use, this project has been able to demonstrate effective techniques to do this for subsequent analysis on different samples.
- The sampling selection and preparation strategy proved effective, and water jet cutting was shown to be particularly suited to this as it did not induce any deformation in the samples. However, sample preparation could potentially generate misleading results if the polishing procedure does not eliminate the deformation due to grinding (as visible in sample B2-3R2).
- The use of electron back scattering diffraction linked to scanning electron microscope showed the most informative results on the characteristics that could be linked to manufacturing or in-service changes.
- More time is required to prepare samples than the 24 hour window on the quayside. This significantly restricted the amount of analysis that was possible.

9 Summary of tripod visual inspection by Blackfish

The inspection work completed by Blackfish is detailed in the sections below. It consists of 4 main areas of work, which are discussed in detail.

- Visual inspection of the tripod, and comparison to the new condition
- Assessment of anodes
- Assessment of the cartridge plate and electrical connectors
- Assessment of different materials

9.1 Visual inspection of the tripod.

To remove the tripod, it was necessary to remove some of the structural members due to the mobile crane lifting capacity. As a result, the top section main tube was cut off whilst the tripod was in the sheltered location. In addition, the main part of the central vertical tube was cut away, as well as some of the horizontal stiffening members were removed.

Lift 1 too heavy

Lift 2 with central vertical member and lower horizontal members removed

Figure 25 - Lifting tripod onto Hatston Quay

Upon removal of the tripod form the water, it was placed on Hatston quay for 24 hours prior to being removed and scrapped., In this short time frame, it was possible to complete some photographic surveys and to remove some components from the cartridge plate for later detailed inspection.

Relevant images are shown below with commentary on specific features that are visible. General observations include:

- Biofouling is extremely heavy in nearly all areas. Very few parts of original steelwork are visible. ICIT noted that biofouling is typical of end-stage' or 'climax' biofouling communities. Thicknesses up to 12cm are present.
- Overall, there does not appear to be a significant directionality effect due to the tidal flow. Growth is relatively even across all areas of the tripod. It has been noted that in sheltered areas there are some different species, most notably sponges

- Biofouling in areas where the water is very stagnant is notably thinner. For instance, in protected areas around the connectors and cartridge plate and inside the main tubes, biofouling is particularly thin (<0,5cm). On the connectors, there is no evidence of large individual species (e.g. barnacles, muscles) but a instead a hard, continuous layer of macrofouling.
- The painted carbon steel surfaces seem to have survived reasonably well. Where biofouling has been scraped away, there is still significant evidence of the black paint. In general, the top section seems to have suffered worse, with random patches of rust covering approx. 25% of the surface area and this may well be due to the increased flow velocity higher from the seabed. Significant biofouling of the main tripod members makes a similar assessment difficult, but where biofouling has been removed the paint seems to be in-tact.
- There is very little evidence of any yellow topcoat paint left.
- The stainless 316L components, including M4-M10 fasteners, have survived well and little corrosion is visible. Some discolouration is present but overall. Fasteners have been unscrewed from their holes rather than needing to be cut off.

The images below provide a good comparison of how the main features have been affected by the 11-year immersion in a tidal site. Obviously, the tripod is very heavily affected by biofouling, up to 12cm thick in places. The biofouling is documented in more detail in ref 1.

Figure 26 - Overview of tripod condition after 11 years

9.2 Assessment of anodes.

Anodes were removed and weighed as part of the inspection procedure by staff at EMEC. The results are shown in Appendix A. In summary, the average anode mass (not including the metal bar) was

21kg, with a range of 17-26kg. The original mass was not defined on the top-level drawing, but from other data it is assumed that each anode was 50kg when it was originally attached.

It is perhaps surprising that any anodes remain after such a long time, but 29 anodes each of 50kg provides a large total of cathodic material to provide protection and is perhaps the main reason why the tripod and paint remains in relatively good condition.

Figure 27 - measuring the mass of anodes by EMEC staff

Photographs clearly show that the sponge species seem to be attracted to the anodes, as can be seen in Figure 28 below. It cannot be confirmed if this has a detrimental effect on the cathodic protection performance of the anodes, but may be something to investigate further.

Figure 28 - condition of anodes after 11 years

9.3 Assessment of the cartridge plate and electrical connectors

Due to the nature of the cartridge plate and electrical connectors with higher numbers of smaller components and different materials, a more detailed assessment was made in this area to assess how the connectors have lasted and the interaction of different materials in close proximity.

A photographic comparison of the cartridge plate is seen in Figure 29. Clearly there is a marked visual difference due to biofouling, but a more detailed study shows that overall the components have survived well, in particular the stainless steel 316L parts including fasteners. Most fasteners were removed easily with hand tools and did not require to be cut or drilled.

Comparison of new and recovered cartridge plate

Figure 29 - Comparison of cartridge plate and connectors

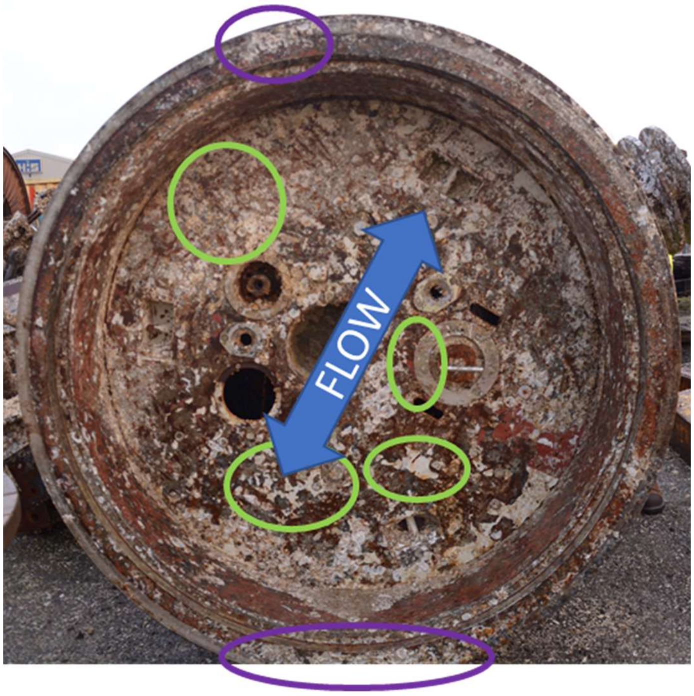

Figure 30 - Tower top with cartridge plate. Green circles indicate remaining paint, purple circles indicate thicker biofouling regions on flange

Key observations:

- It is notable in comparison to the tripod that the paint on the cartridge plate has almost entirely disappeared. Some of the paint may well have been removed during the scraping of the biofouling from the cartridge plate as there are indications of mechanical biofouling removal but there is significant indications of corrosion on much of the plate, indicating the paint had fallen off whilst it was still submerged. Unfortunately, it is not possible to provide a conclusion of the root cause of paint removal.

9.3.1 Tower top flange

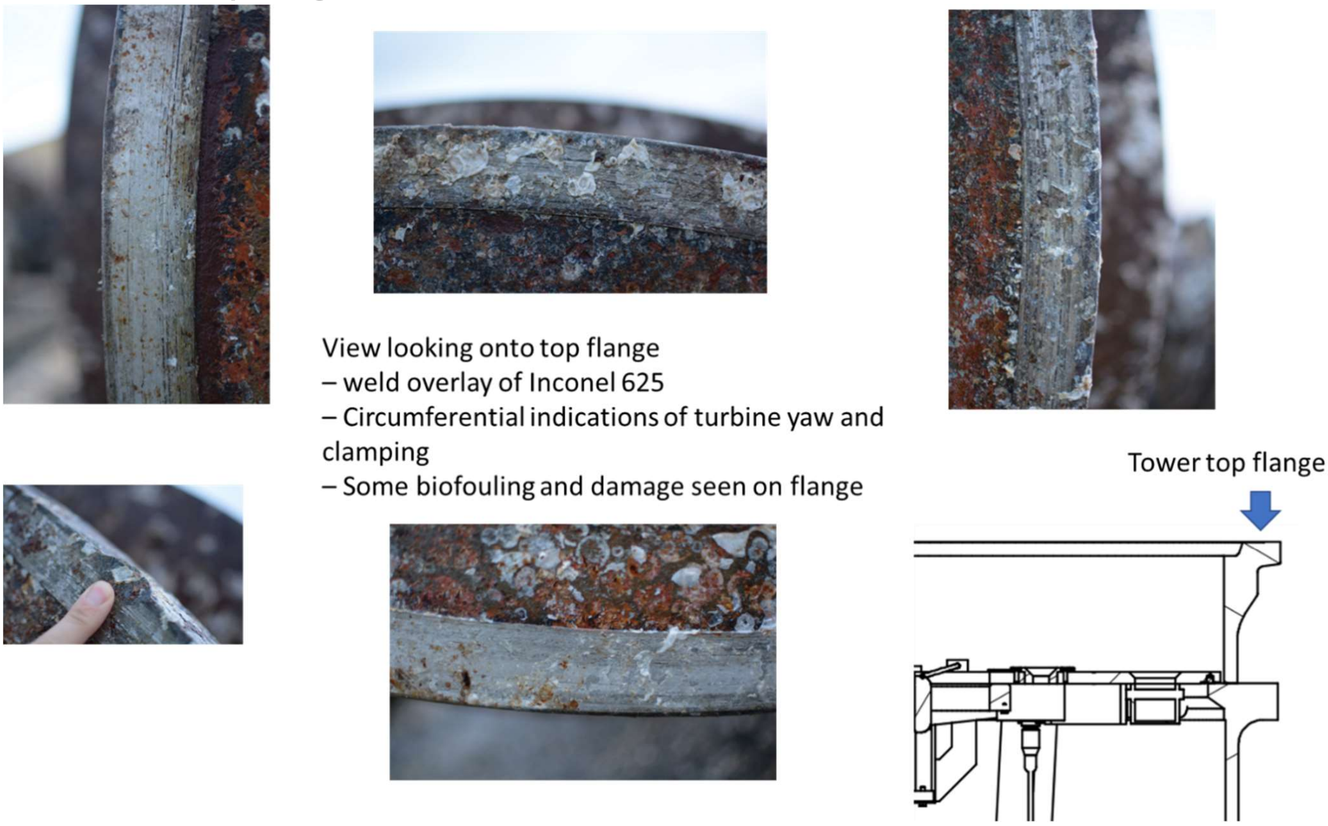

Figure 31 - View of tower top flange

Inspection of the tower top flange was completed, as this was an important feature of the TGL turbine. The yawing turbine used this flange surface as a yawing bearing surface between tides, but during generation this surface was used to create friction that enabled reaction of yawing moments into the foundation. It is a carbon steel flange with a weld overlay of Inconel 625.

Key observations:

- Circumferential marks are present from both machining marks and also where the turbine used this as a yawing bearing surface.
- There is no particular location that show greater wear than others
- There is indication that biofouling is more prevalent in one direction, which correlates to approx. 60 degrees from the flow direction (purple circles in Figure 30). No particular conclusion can be drawn from this relating to the flow direction and prevalence of biofouling, given the lack of evidence from the tripod structure.

9.3.2 Diamould high power connector

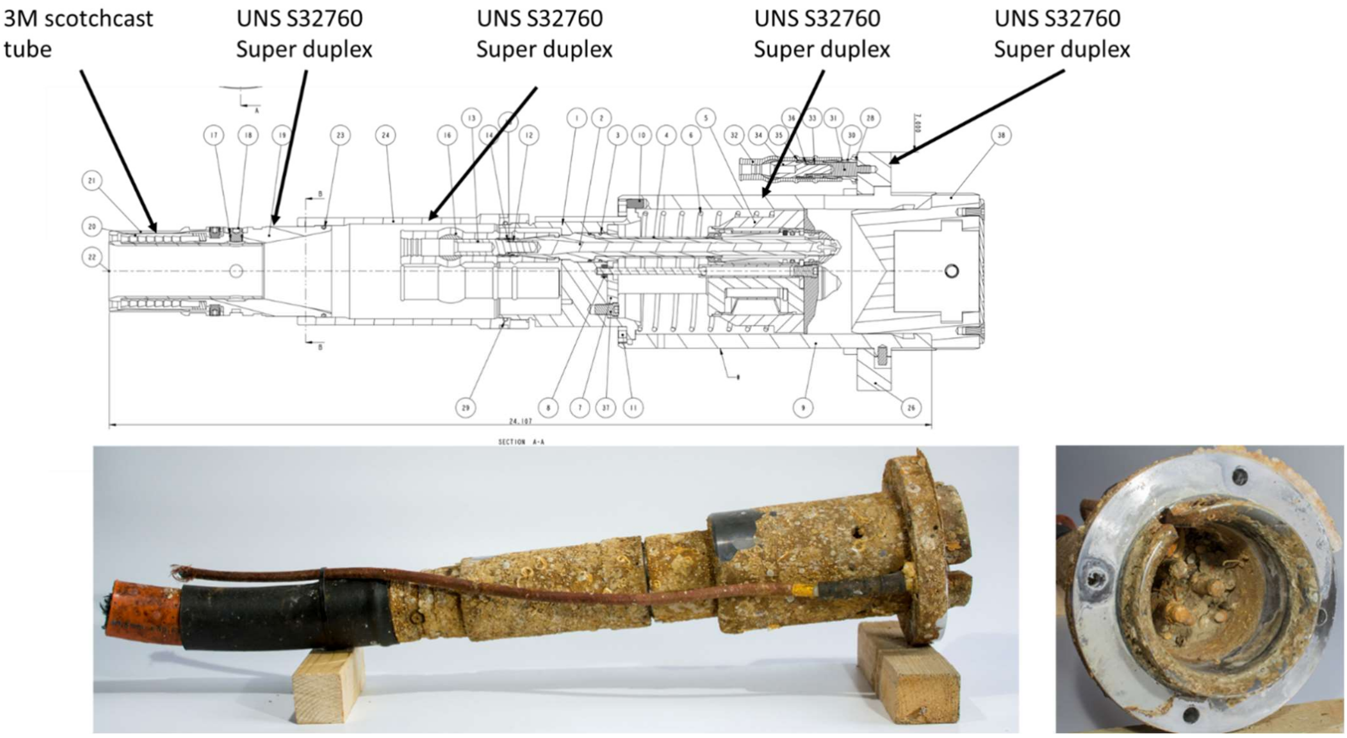

Figure 32 - Assessment of Diamould power connector

Key observations:

- Super duplex stainless steel has resisted corrosion well, but is not immune to biofouling.
- The synthetic compounds (3M Scotchcast and HDPE) are very resistant to biofouling
- The pins of the connector show signs of corrosion, but this connector was exposed to seawater for prolonged periods of time throughout its lifetime. The ROV cap was not properly in place, and it was clear when this was removed that there was significant biofouling inside the top of the connector. Proper and timely connector capping would have likely reduced this considerably.

9.3.3 Seacon fibre optic connector

Figure 33 - assessment of Seacon fibre optic connector

Key observations

- The titanium surfaces are not immune to biofouling, but once scraped off it is apparent that the titanium surface is undamaged
- There is no apparent corrosion on the titanium surfaces
- Rubber and HDPE materials are biofouling resistant.
- One of the major concerns during build was the use of M4 bolts to clamp the connector to the flange. This was impossible to change at the time. However, it is apparent that even these small bolts have survived well and there is little evidence of corrosion, thread damage or even discolouration.
- The tip of the connector appears to have biofouling on it – this is likely due to the fact that the ROV cap was not installed correctly.
- It was very difficult to remove the stainless mounting bucket through the cartridge plate as the biofouling prevented it coming through the near size for size hole.

9.3.4 Other small components

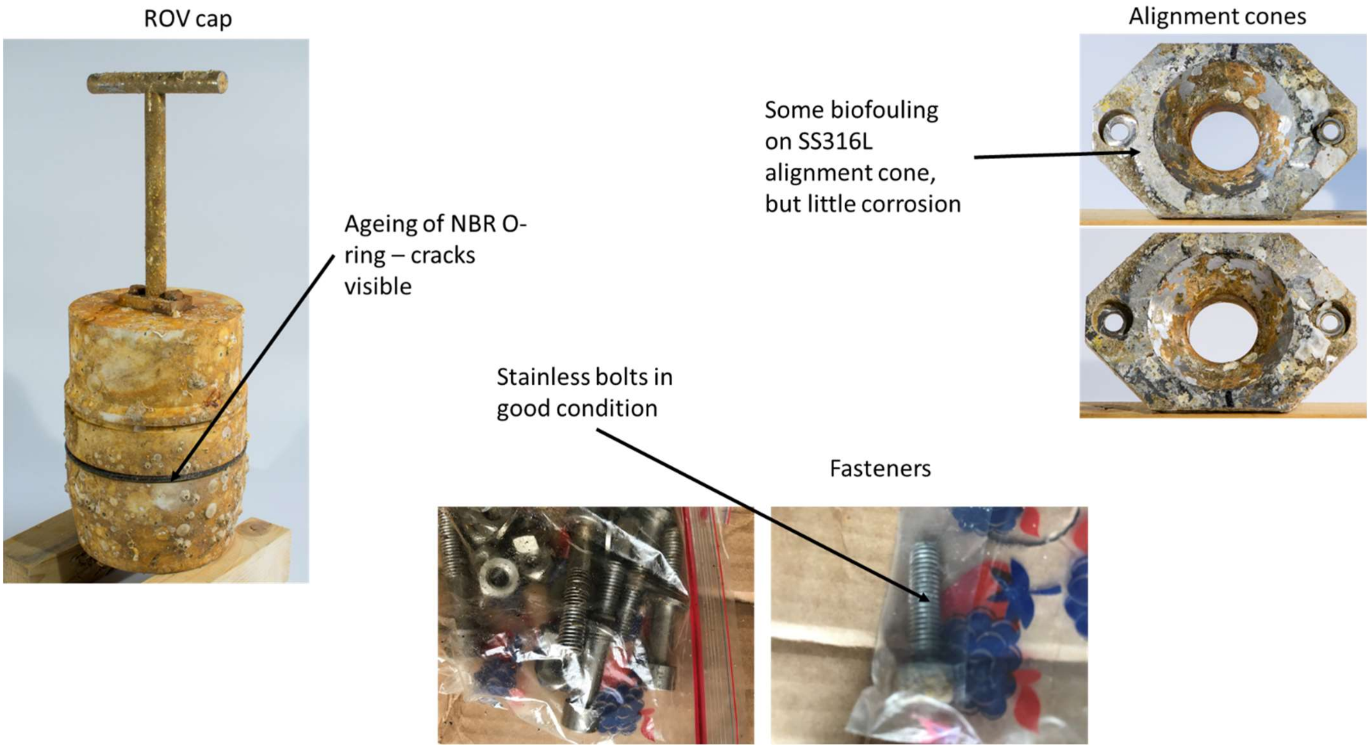

Figure 34 - Assessment of other small components on the cartridge plate

Key observations

- Stainless fasteners have survived very well, even those exposed to the tidal stream on the top of the cartridge plate.
- The NBR O-ring material has shown signs of ageing and cracking. It is not clear what conditions have caused this as the history of the part is not known. UV, temperature, and long term exposure to seawater can all cause ageing effects.
- The yellow plastic connector cap has more biofouling compared to the connector hoses. Examples of mature barnacles are present.
- SS316L alignment cones have survived well, with little corrosion. Some biofouling is present, particularly on the upper surface exposed to the tidal flow.

9.3.5 Tripod tower top internal volume

The internal volume below the cartridge plate is where the cabling from the connectors is managed and the crossover box installed. Figure 35 shows the condition of these components.

Figure 35 - Cartridge plate internal features

Key observations:

- Condition of these components is generally quite good. Paint has survived well under the biofouling
- Levels of biofouling are significantly lower than seen on external surfaces.
- Cables, cable sheaths and cable ties are in excellent condition.
- It is worth noting that the ROV connector cap was found loose in this volume. This is photographed in Figure 34 where O-ring cracking can be seen. It is possible that this was lost up to 10 years ago and the O-rings have been left exposed to seawater for the entire deployment time, hence the ageing and cracking.

9.4 Summary of material performance

Below is a list of materials that have been used and inspected, with comments on how it has survived the 10 years of sub sea immersion:

<u>Painted Carbon Steel:</u> generally good where paint is still attached. Heavy corrosion where paint is flaking away and this seems to be common where there are bolt holes or edges that initiate paint cracking.

<u>Stainless Steel 316L (1.4404</u>). Most of these parts have survived extremely well, in particular the stainless steel fasteners. Most of these are M8-M12 and screwed into carbon steel components. There is very little evidence of corrosion on the threads or bolt heads. At the time of assembly, it was necessary to use M4 fasteners for the fibre optic connector flange to the mounting flange and there were concerns about this. However, these fasteners have survived very well and were removed using hand tools only.

Titanium: This is used on the body of the fibre optic connector. Some thin biofouling crust is visible on much of this, but where this has fallen off during handling, the titanium surface is virtually unblemished and as good as new. Titanium is recognised as a very inert material and this provides evidence to confirm this. Biofouling has attached itself to much of the material in a thin layer, but the lack of significant biofouling is probably due to the fact that the connector is in stagnant, dark water there is little growth.

Polyurethane hose sheathing: This has survived well with little biofouling. There is no particular indication of material degradation.

Plastic and rubber (detailed spec unknown): in general, non-metallic materials have survived well. There is some indication of cracking on the NBR O-rings that hold in the ROV connector cap. Cable outer sheath (likely HDPE) and over mouldings show no signs of ageing and little in the way of fouling. It should be noted that there would have been no daylight in this location (under the cartridge plate) and little water flow.

10 Conclusions and Lessons learned

Lessons learned and recommendations for future marine renewables devices:

- It is clear that every surface that is exposed to seawater, no matter how high the current, will be subjected to vigorous fouling. Certainly, components that are expected to move, slide, or require clearance in any way must be designed assuming that biofouling will occur on all steel surfaces.
- Epoxy paint seems to have performed reasonably well despite the biofouling. There are some areas where paint has peeled away, but these seem to be predominantly close to features with corners, holes, edges or features that provide a paint crack initiation site.
- Different coloured paint was used for installation purposes to be able to use ROVs to provide visual feedback. However, after years of being submerged, there is no evidence of the paint colours nor any identification marks. Even after a short time (2 years) paint identification marks (colours or text) were totally indistinguishable to an ROV.
- Biofouling up to 12cm thick has been seen, resulting in additional mass of 14kg/m2. This may need to be accounted for in designs that are particularly sensitive to buoyancy or mass and for lifting equipment calculations.
- Biofouling is markedly reduced where there are surfaces that are totally dark or in stagnant water.
- SS316L, titanium and super duplex material have all shown excellent resistance to corrosion, but all of them are susceptible to biofouling.
- SS316L fasteners have performed extremely well. This grade of stainless is commonly known as marine grade stainless, but corrosion can occur particularly in poorly cathodically protected areas or where there are large discrepancies in surface area of materials. However, in all cases for parts on the tripod, the stainless fasteners have survived well, with little or no evidence of corrosion on bolt heads or threads. All fasteners were removed by hand with little trouble.

- For maintenance, biofouling thickness should be considered. Given how hard it is to remove, sliding components through near size for size holes can be very difficult. Include an allowance for biofouling build up.
- Components that are installed for long term submersion should account for biofouling end stage communities, with thicknesses up to 15cm.
- An increase in lifting capability of up to 14kg/m2 must be accounted for if components are to be submerged for many years. This can be reduced if components are recovered in a shorter time period.

Lessons learned associated with the provision of the inspection services include:

- Diver surveys need to be completed in static water.
- Diver surveys need to be done as soon as possible, to prevent the growth of new biofouling species.
- More time is required on site to assess biofouling than the 24-hour window provided.
- The ROVCO scanning tool is an excellent method of providing advance knowledge of the condition of subsea hardware. ROV surveys can be difficult to interpret and the exact view of a feature of interest is not always possible. In particular it can be difficult to get good resolution still images from the video.
- Preliminary measurements of biofouling thickness can be taken from the point cloud data and correlate well with actual measurements.
- The sampling selection and preparation strategy proved effective, and water jet cutting was shown to be particularly suited to this as it did not induce any deformation in the samples. However, sample preparation could potentially generate misleading results if the polishing procedure does not eliminate the deformation due to grinding.
- The use of electron back scattering diffraction linked to scanning electron microscope showed the most informative results on the characteristics that could be linked to manufacturing or in-service changes.
- More time is required on site to prepare samples than the 24-hour window for this project

Appendix A: Anode mass results

Anode No.	Mass / kg	Mass w/o bar / kg
1	26	21
2	31.5	26.5
3	24.5	19.5
4	23.5	18.5
5	25.5	20.5
6	25	20
7	23.5	18.5
8	27	22
9	25.5	20.5
10	23	18
11	25.5	20.5
12	30.5	25.5
13	26	21
14	27	22
15	25	20
16	26.5	21.5
17	27.5	22.5
18	25.5	20.5
19	25.5	20.5
20	23	18
21	23	18
22	30.5	25.5
23	27	22
24	31.5	26.5
25	23.5	18.5
26	25	20
27	24	19
28	25.5	20.5
29	22.5	17.5
total / kg	749.5	604.5
average / kg		20.8
max / kg		26.5
min / kg		17.5

11 Appendix B: Large format pictures

Figure 36 - Large version of biofouling samples

Figure 37 - Large version of ROVCO point cloud model

Figure 38 - Large version - tripod leg

Figure 39 - Large version - tripod node

Figure 40 - Large version - tripod node

Figure 41 - Large version - tower top flange 12 and 6 o'clock positions

Figure 42 - Large version tower flange 9 and 3 o'clock positions

Figure 43 - Large version Diamould power connector pins

Figure 44 - Large version Diamould power connector

Figure 45 - Large version Seacon fibre optic connector

Figure 46 - Large version Seaon fibre optic connector end view

Figure 47 - Large version Seacon fibre optic connector end

Figure 48 - Large version Alignment cone